

See discussions, stats, and author profiles for this publication at: <https://www.researchgate.net/publication/231674845>

# Sealed Minitrough for Microscopy and Long-Term Stability Studies of Langmuir Monolayers

ARTICLE *in* LANGMUIR · DECEMBER 2002

Impact Factor: 4.46 · DOI: 10.1021/la026372y

---

CITATIONS

16

---

READS

27

3 AUTHORS, INCLUDING:



[Ka Yee C. Lee](#)

University of Chicago

**157** PUBLICATIONS **3,935** CITATIONS

[SEE PROFILE](#)



[Jacob Israelachvili](#)

University of California, Santa Barbara

**282** PUBLICATIONS **19,719** CITATIONS

[SEE PROFILE](#)

# Sealed Minitrough for Microscopy and Long-Term Stability Studies of Langmuir Monolayers

Yufang Hu,<sup>†</sup> Ka Yee C. Lee,<sup>‡</sup> and Jacob Israelachvili<sup>\*,†</sup>

Department of Chemical Engineering, University of California, Santa Barbara, California 93106, and Department of Chemistry, Institute for Biophysical Dynamics and James Franck Institute, University of Chicago, Chicago, Illinois 60637

Received August 8, 2002. In Final Form: October 16, 2002

We report the design and calibration of a miniature Langmuir trough that can be mounted on a microscope stage. The fully sealed trough can be used for carrying out routine monolayer experiments, such as the control and measurement of area and surface pressure, on the order of 13 h without infiltration of contaminants. In experiments carried out with the minitrough to observe the slow growing and shrinking of monolayer domains via the Ostwald ripening process, qualitative observations and quantitative results were in good agreement with theoretical expectations. The minitrough can also be used to study biological amphiphiles (e.g., lipid–protein interactions) in controlled vapor and under contaminant-free conditions.

## Introduction

Langmuir monolayers and Langmuir–Blodgett (LB) films have been used extensively for studying the interactions of surfactants, lipids, proteins, and model cell membranes.<sup>1</sup> Since the inception of the original trough by Agnes Pockels<sup>2,3</sup> more than 100 years ago, a wide variety of troughs have been designed for different types of measurements of monolayer properties and for depositing monolayers on solid surfaces,<sup>1</sup> and the more recent introduction of sophisticated imaging techniques<sup>4–7</sup> has further catalyzed research activities in this area. In many of these studies, the need to study the surface properties of biological molecules that are easily degradable and slow to equilibrate calls for a completely clean, that is, fully sealed, trough that still allows for normal pressure–area measurements to be made over long time periods. Such a trough should have a small surface area because of the limited quantity of experimental material available. In addition, the trough should be able to be used in conjunction with a fluorescence microscope for optical imaging.

This paper describes the design and performance of a miniature trough, or “minitrough” (Figure 1), that meets the above criteria. The trough was originally designed for fluorescence microscopy studies of lipid monolayers over long periods of time, ranging from minutes to days, to establish their “true equilibrium” properties and microstructure, such as the domain size and shape. To successfully carry out these experiments, the issues of water evaporation and contamination, that is, environmental control and cleanliness, have to be addressed. To this end, we designed a trough that keeps the monolayer and the liquid subphase fully sealed from the outside environment

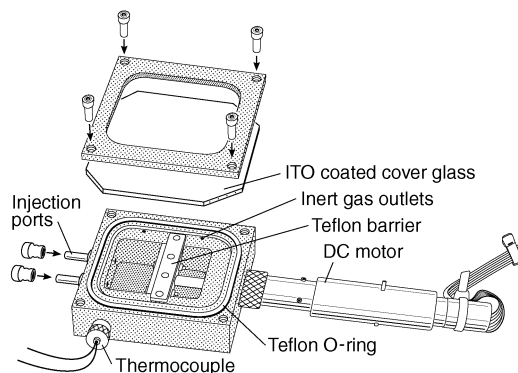


Figure 1. Schematic of the minitrough.

using a gas-tight Teflon O-ring. The size of the trough was kept small so that the entire unit could be rested on the translation stage of a fluorescence microscope or other optical microscopes. The small trough size and surface area (approximately 16 cm<sup>2</sup>) are also convenient for studies of materials of limited quantities. The requirement of a sealed minitrough having a very small gap between the water–vapor interface and the viewing window renders it difficult to use a conventional surface pressure measuring technique, such as the Wilhelmy plate method. A novel alternative method was therefore adopted where the elastic deformation of a small, planar hydrophobic wire loop, resting on the water surface, was used to quantify the surface pressure. The details of a sample experiment using the minitrough are given in this paper.

## Materials and Methods

This section describes the setup of the fluorescent microscope, the design and construction of the minitrough, and the “wire loop tensiometer” for surface pressure measurements.

**Fluorescence Microscopy Imaging.** All fluorescence microscopy experiments were conducted using the setup as shown in Figure 2. A Nikon Eclipse E800 fluorescence microscope (Nikon Inc., Instrument Group, Melville, NY) was used for imaging. The fluorescence images from the microscope were fed to an image-intensified CCD camera (Cohu Inc., San Diego, CA) directly connected to the microscope. The black-and-white fluorescence images were recorded using a VCR (Panasonic, super

<sup>†</sup> University of California.

<sup>‡</sup> University of Chicago.

(1) Gaines, G. J. *Insoluble Monolayers at Liquid–Gas Interfaces*, 1st ed.; John Wiley & Sons: New York, 1966.

(2) Pockels, A. *Nature* **1891**, 43, 437–439.

(3) Pockels, A. *Nature* **1893**, 48, 152–154.

(4) McConnell, H. *Annu. Rev. Phys. Chem.* **1991**, 42, 171–195.

(5) Ding, J.; Takamoto, D.; von Nahmen, A.; Lipp, M.; Lee, K.; Waring, A.; Zasadzinski, J. *Biophys. J.* **2001**, 80, 2262–2272.

(6) Evert, L.; Leckband, D.; Israelachvili, J. *Langmuir* **1994**, 10, 303–315.

(7) Baneyx, G.; Vogel, V. *Proc. Natl. Acad. Sci. U.S.A.* **1999**, 96, 12518–12523.



**Figure 2.** Experimental setup of the minitrough on the fluorescence microscope.

VHS). Video images were digitized using All-In-Wonder software (128 PCI 32 MB video card, ATI Technologies, Inc., Ontario, Canada) on a PC.

To calibrate the wire loop (described below), a commercial ribbon trough (Joyce-Loebl Langmuir Trough IV, U.K.) with a built-in pressure sensor was used. The deformation of the wire loop was recorded using a CCD camera (Pulnix TM200, America Inc., Sunnyvale, CA). The video images were analyzed using the same procedure as outlined above.

**Design and Construction of the Minitrough.** The trough (Figure 1) dimensions are 8.4 cm (length)  $\times$  3.5 cm (width)  $\times$  3.3 cm (height). The maximum water surface area is 16.0 cm<sup>2</sup> (4.5 cm  $\times$  3.5 cm) and the compression ratio is approximately 4, leaving 4 cm<sup>2</sup> for the pressure-measuring wire loop tensiometer (to be described in the following section). The trough chamber was machined from 316 stainless steel, which is corrosion resistant. The interior surface of the trough was coated with a thin hard layer of Teflon for inertness (Crest Coatings, Anaheim, CA). The Teflon coating covers most of the stainless steel surface of the trough that comes into contact with the aqueous subphase during an experiment. A few interior holes and channels, however, could not be reached by the coating process. The exposed surfaces of these holes were shielded from the subphase by a metal oxide layer created by the acid passivation procedure described below. This combination takes advantages of the structural support provided by stainless steel and the inertness of the Teflon coating. The trough chamber and all the other stainless steel parts were periodically disassembled and passivated in nitric acid solution (30% w/w) at 60 °C for 30 min. The passivation creates an impermeable metal oxide layer on the 316 stainless steel surface that prevents the leaching of metal ions into the subphase during experiments.

The movable Teflon barrier was milled from a solid block of virgin Teflon. A dc motor (Micro Electronics, Inc., Seekonk, MA) controls the movement of the barrier. The motor and barrier were connected via an O-ring-sealed stainless steel shaft. The position of the barrier is tracked by a digital encoder (Newport Corp., Irvine, CA). To avoid leakage around the barrier, a very snug fit between the Teflon barrier and the inner surfaces of the trough is needed. This is achieved through applying an even radial distribution of compressive pressure at contact areas by having the Teflon barrier compressed in both the normal and horizontal directions. The Teflon barrier becomes deformed or worn with use and needs to be replaced every few months.

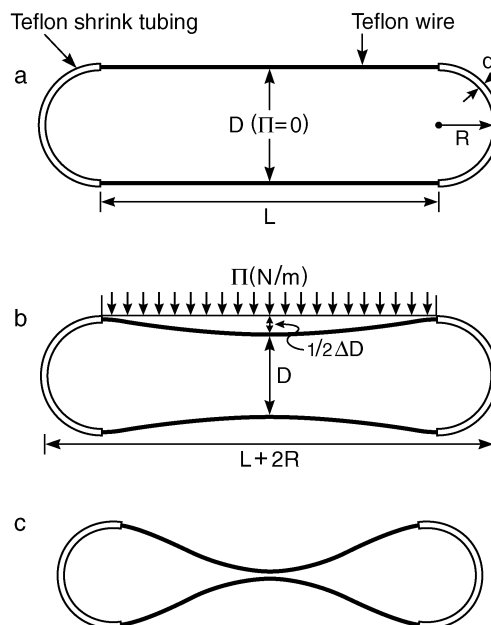


**Figure 3.** Schematic of the wire loop tensiometer. (a) The undeformed wire loop when no external load is applied. (b) The wire loop under a small load. The straight portions of the wire loop begin to deform. No visible degree of deformation on the bent portions can be observed. (c) The wire loop undergoing a large deformation. The deformation of the bent portion causes the wire loop to shorten.

The water surface of the trough is isolated from the external environment by a gas-tight Teflon O-ring seal. A 0.7 mm thick piece of indium–tin oxide (ITO) coated cover glass (resistance  $\sim 20 \Omega$ ) is fastened down on the trough base. The cover glass is pressed down with a rectangular steel frame onto the main O-ring on the trough base. A weak current is passed through the ITO coating to resistively heat the glass to prevent water vapor from condensing on the cover glass during experiments.

A few attachments or feedthroughs have been added to the trough to increase its versatility (cf. Figure 1): (1) A small thermocouple in direct contact with the subphase records the subphase temperature. (2) Two injection ports attached to one end of the trough allow the subphase contents to be varied during an experiment without having to remove the trough cover. (3) Small gas inlet/outlet holes drilled through the trough walls allow for flushing the chamber or changing the gas in contact with the monolayer. A hollow needle (not shown in Figure 1) can be manipulated from the outside to aspirate different regions of the interface, for example, to periodically sweep clean the interface inside the wire loop. All feedthrough ports are sealed via Teflon O-rings and plugs.

**Wire Loop Tensiometer for Surface Pressure Measurements.** The need to have the glass cover close to the water surface renders the usage of conventional surface pressure measuring devices, such as the Wilhelmy plate, difficult, because these devices are bulky yet would need to be fully contained inside the small trough. To meet this requirement, we substituted the Wilhelmy plate with a small hydrophobic wire loop constructed from ultrathin Teflon wire (Figure 3a). The planar rubber-band-shaped loop is closed at both ends and floats on the air–water interface.

When certain approximations are applied, the deformation of the wire loop can be calculated using the equation for a uniformly loaded cantilever beam clamped rigidly at one end:<sup>8</sup>

$$x = \frac{wL^3}{8EI} \quad (1)$$

(8) Greenwood, D. *Engineering data for product design*; McGraw-Hill: New York, 1961.



where  $x$  is the maximum deformation of the cantilever beam;  $w$  is the total load on the cantilever beam in units of force;  $L$  is the length of the cantilever beam;  $E$  is the Young's modulus or elastic modulus of the beam material, which is approximately 1.1 GPa for Teflon;  $I$  is the moment of inertia of the beam. For a beam having a circular cross section such as the Teflon wire used here,  $I = \pi d^4/64$ , where  $d$  is the diameter of the circular cross section of the beam.

For the case of the wire loop deforming under an applied surface pressure  $\Pi$ , the above equation can be modified as

$$\frac{\Delta D}{2} = \frac{\Pi(L/2)^4}{8EI} \quad (2)$$

where  $\Delta D$  is the difference in the distance between the geometric centers of the two straight arms of the wire loop,  $D_0 - D(\Pi)$ .  $D_0$  is the distance when the wire loop is undeformed, and  $D(\Pi)$  is the distance when the wire loop is deformed in the presence of a Langmuir monolayer with a given surface pressure.

Equation 2 indicates that the deformation of the wire loop is linear with respect to the surface pressure of the monolayer. Thus, if a calibration is made prior to measurement and the relationship between deformation and surface pressure is known, the wire loop can be used as a tool for the measurement of surface pressure of a Langmuir monolayer.

The physical size of the wire loop was determined experimentally to meet the required sensitivity and measurement range. As shown in Figure 3a, the dimensions of the final undeformed wire loop are  $R = 2.5$  mm and  $L = 27$  mm. The final version of the wire loop was made of one piece of Teflon wire with cross-sectional diameter  $d = 192$   $\mu\text{m}$  (Zeus Inc., Orangeburg, SC) and two pieces of Teflon heat shrink tubing with wall thickness of  $0.0025 \pm 0.0005$  in. and inside diameter of  $0.003 \pm 0.0005$  in. (Zeus Inc.). The wire loop was made by positioning the two pieces of heat shrink tubing symmetrically at the bent ends of the loop and applying heat. The heat shrink tubings were pressed against cylindrical metal rods for shaping while being heated.

To experimentally calibrate the deformation of the wire loop, the loop was laid down on the clean water surface of a conventional trough, and a dimyristoyl-phosphatidyl-ethanolamine (DPPE) monolayer was spread on the air–water interface. The monolayer was slowly compressed and then expanded. Surface pressure was measured using a Wilhelmy plate attached to the trough. The loop was video recorded during the entire process, and the recorded images were later downloaded from the video and processed using Adobe Photoshop to measure the change in loop dimensions as a function of the applied pressure. The results are given in Results and Discussion.

**Experimental Procedure.** Dimyristoyl-phosphatidyl-choline (DMPC) and DPPE were purchased in powder form from Avanti Lipids (Birmingham, AL). Dihydrocholesterol (DChol) was purchased from Sigma. The fluorescent dye Texas Red, 1,2-dihexadecanoyl-*sn*-glycero-3-phosphoethanolamine, triethylammonium salt (Texas Red), was purchased from Molecular Probes (Eugene, OR). All chemicals were used without further purification.

Prior to each experiment, the trough was thoroughly cleaned with chloroform and acetone and rinsed with Milli-Q water. For the Ostwald ripening experiment, the chloroform spreading solution consisted of 10% DChol, 89.5% DMPC, and 0.5% Texas Red in molar ratio. The trough was set at maximum barrier expansion during monolayer deposition. Approximately 10 min was allowed for the organic spreading solvent to evaporate. The trough was then sealed and kept sealed for the remainder of the experiment. The monolayer was first compressed at a steady speed until the mixing–demixing line was crossed, turning the biphasic film into a homogeneous one (Figure 4a–b–c). The monolayer was then left to equilibrate until the two contrasting phases disappeared and the fluorescent field appeared to be completely homogeneous (Figure 4c). After an apparent one-phase state was reached, the monolayer was then expanded to the targeted two-phase state. This compression/expansion procedure ensured a reproducible initial condition for each experiment. The monolayer was held at the target pressure for an

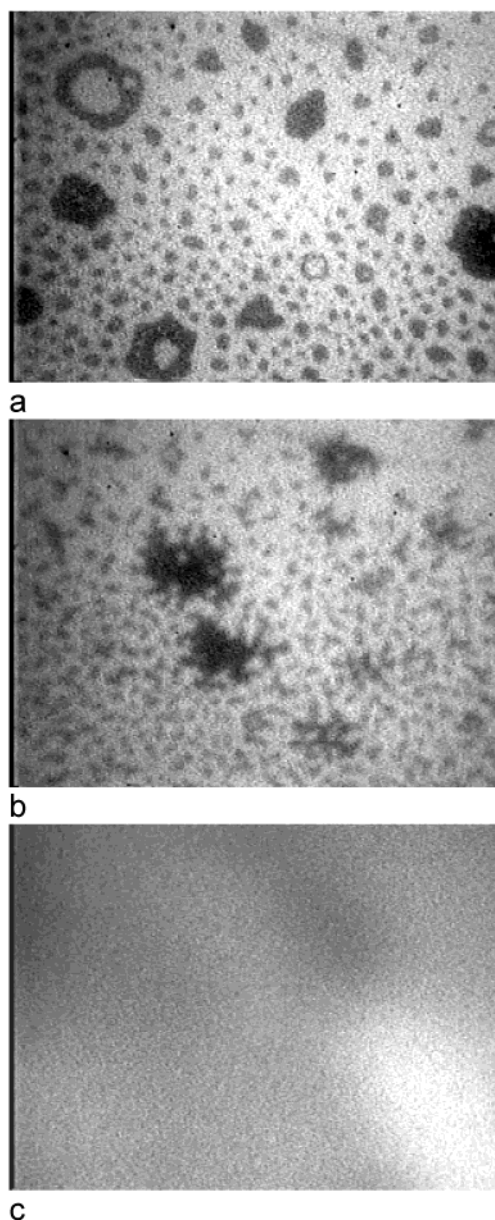


**Figure 4.** Monolayer domains during compression. (a) The onset of phase transition marked by fluctuations of the domain boundaries. The dark domains are the DChol-rich phase, and the bright background is the lipid-rich phase. (b) The phase separation proceeds as the surface pressure further increases. (c) Completion of the phase separation. The entire monolayer is now in a one-phase state (refs 4 and 16).

extended period of time while the domain sizes and morphology were video recorded.

## Results and Discussion

**Calibration of the Wire Loop Tensiometer.** The microscope images of Figure 5 show the wire loop at surface pressures of  $\Pi = 0$ , 10.9, and 26.0 mN/m. The deformation of the loop with increasing pressure is clearly visible and measurable. To test the hysteresis in the loop, two complete compression/expansion cycles were carried out, as shown in Figure 5. The relationship between deformation and surface pressure is strongly linear over the range measured, which is in agreement with eq 2. The measured displacement–pressure line has a mean slope of  $dD/d\Pi = 0.09$  mm/(mN/m), which may be compared with the value of 0.113 mm/(mN/m) obtained using eq 2.

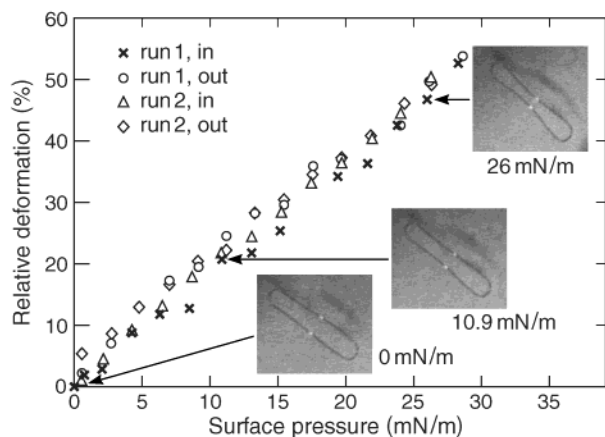


**Figure 5.** Measured deformation of the wire loop as a function of surface pressure.

In reality, when the wire loop is being compressed, the external load is distributed throughout the entire loop. The overall deformation is a summation of the deformations from the straight and the bent portions of the wire loop. At large loads, the contribution of the bent portions of the loop becomes more significant; meanwhile, the end-to-end distance of the loop shortens (Figure 3c). Apparently, to accurately represent the deformation of the loop, all of these modes have to be taken into account. In light of these arguments, the result obtained using eq 2 is a satisfactory approximation to the actual scenario and sufficient for designing loops having the desired characteristics.

The measurement limit of the wire loop can be calculated as well. This theoretical value is taken to be the smaller of the two values as determined by the elastic limit of Teflon and the physical size of the wire loop.

When the load on the wire loop exceeds the mechanical limit of Teflon, its deformation deviates from the linear elastic regime. This elastic limit can be estimated theoretically by equating the tensile strength,  $\sigma_{\max}$ , of Teflon with the maximum normal stress at the cross section:<sup>9</sup>

$$\sigma_{\max} = \frac{M_{\max} d/2}{I} \quad (3)$$

where  $M_{\max}$  is the maximum moment of a given beam geometry. For a cantilever beam under uniform load,<sup>9</sup>

$$M_{\max} = \frac{\Pi_{\max, \text{elastic}} L^2}{8} \quad (4)$$

When these two equations are combined, the maximum allowable surface pressure that can be measured in the elastic regime is expressed as

$$\Pi_{\max, \text{elastic}} = \frac{\pi d^3 \sigma_{\max}}{4L^2} \quad (5)$$

Taking the tensile strength of Teflon to be  $1.7 \times 10^7 \text{ N/m}^2$  (Zeus Inc., technical menu), the elastic limit of the beam is calculated to be  $\Pi_{\max, \text{elastic}} = 130 \text{ mN/m}$  using eq 5 above, which is well beyond the value for most experimental systems. Below this value of surface tension, the deformation of the wire loop varies linearly as the monolayer surface tension changes.

(9) Gere, J.; Timoshenko, S. *Mechanics of Materials*, 4th ed.; PWS: Boston, MA, 1997.

The physical size of the wire loop sets another limit on the maximum possible deformation of the wire loop. The maximum value of surface pressure that can be measured is determined by the maximum bending possible for the wire loop. Given the undeformed wire loop size of  $R = 2.5 \text{ mm}$ ,  $L = 27 \text{ mm}$ , and  $d = 192 \mu\text{m}$ , the working range of the wire loop is measured experimentally to be 0–60 mN/m.

The scatter in the data points indicates that the tensiometer exhibits some nonlinearity as well as hysteresis, most likely due to the sole use of Teflon in the fabrication of the wire. The error during image analysis contributes to 0.25–0.5% of the measurement. This translates to an error of about  $20 \mu\text{m}$  in the displacement measurement. The error on imaging resolution could be improved by using a more sophisticated camera and image analysis system. Theoretically, this resolution can approach that of the optical limit of  $1 \mu\text{m}$ . A differently fabricated loop, consisting of hydrophobized “spring wire” such as “piano wire” or heat-treated “beryllium–copper” with a thin hard hydrophobic coating, should attain the theoretical performance specifications as calculated in Materials and Methods.

The smallest surface pressure measurable using the current setup can be calculated as a ratio between the resolution of the displacement measurement and the effective spring constant. The experiment values for these are  $20 \mu\text{m}$  and  $0.09 \text{ mm}/(\text{mN/m})$ , respectively; therefore, the smallest measurable surface pressure is  $0.22 \text{ mN/m}$ .

**Performance of the Minitrough.** The focus of our initial study using the sealed minitrough was to study the slow evolution of monolayer domains of the binary DMPC/DChol system. DChol was chosen as a substitute for cholesterol due to concerns of the oxidation of the latter. These two molecules are important building blocks of biological membranes, the one being a flexible molecule (with the acyl chains in the fluid state) and the other a rigid steroid at physiological temperatures. A binary mixture of DMPC/DChol thus serves as an ideal system for studying the phase behavior of biological lipids. Several previous studies on the dynamics and phase behavior of mixed DMPC/cholesterol monolayers have been reported,<sup>10–16</sup> and the complete phase diagram of this system has been constructed by a combination of pressure–area measurements and epifluorescence microscopy.<sup>10</sup> The mixed monolayer apparently exhibits a miscibility gap and separates into a DMPC-rich and a cholesterol-rich phase at pressures above  $\sim 0.5 \text{ mN/m}$  at  $23.5^\circ\text{C}$ , with an upper critical point at a cholesterol concentration of  $\sim 30 \text{ mol } \%$  and a temperature of  $23.5^\circ\text{C}$ .<sup>10</sup>

In all of the above-mentioned studies, true “thermodynamic” phase separation was not attained. If this process is a precursor to a two-dimensional phase separation, that is, via the nucleation and growth of the domains, these domains would be expected to change their size with time until a single macroscopic “domain” or continuous phase remained, in equilibrium with another macroscopic phase. No such growth has yet been reported for monolayer domains on the air–water interface when studied over time periods of hours, although a slow and limited growth of LB-deposited domains on a solid surface via Ostwald

(10) Hirshfeld, C. L.; Seul, M. *J. Phys.* **1990**, *51*, 1537–1552.

(11) McConnell, H. *Proc. Natl. Acad. Sci. U.S.A.* **1996**, *93*, 15001–15003.

(12) McConnell, H.; De Koker, R. *Langmuir* **1996**, *12*, 4897–4904.

(13) Sagui, C.; Desai, R. *Phys. Rev. Lett.* **1995**, *28*, 557–563.

(14) Seul, M.; Andelman, D. *Science* **1995**, *267*, 476–483.

(15) Seul, M.; Morgan, N. Y.; Sire, C. *Phys. Rev. Lett.* **1994**, *73*, 2284–2287.

(16) Seul, M.; Sammon, M. J. *Phys. Rev. Lett.* **1990**, *64*, 1903–1906.



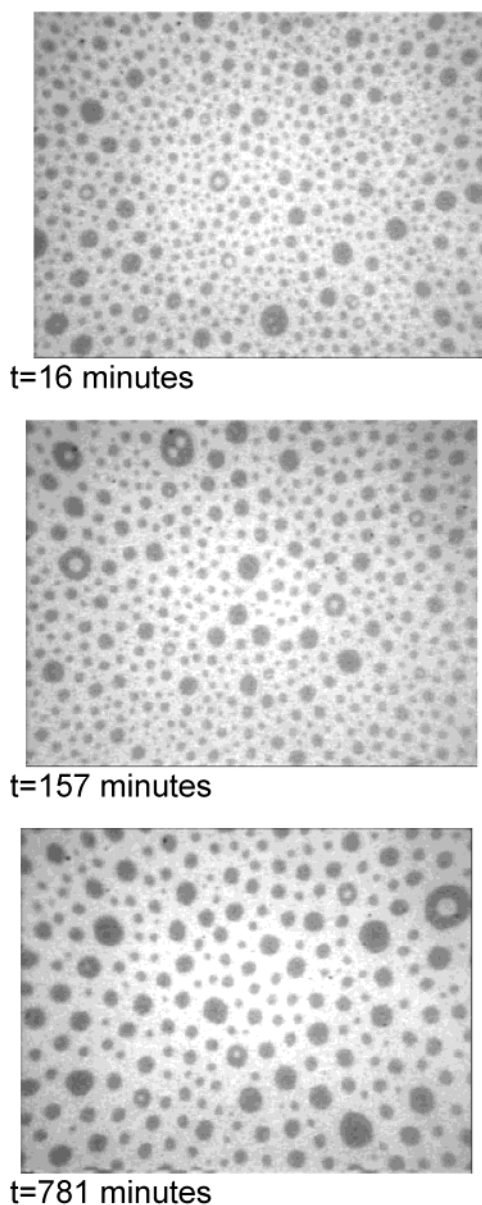


**Figure 6.** Ostwald ripening of the monolayer domains:  $t = 16$  min (0.27 h),  $t = 157$  min (2.6 h), and  $t = 781$  min (13.0 h).

ripening over periods of many hours has been observed.<sup>6</sup> On the other hand, it has been shown that finite-sized microscopic domains could be equilibrium structures due to a balance of long-range repulsive electrostatic-dipole and attractive line-tension forces.<sup>11–16</sup> These domains would be expected to equilibrate at a particular shape and size or radius (ranging from nanometers to microns) at a given surface pressure. Toward the end of our experiment, the domain structures were still slowly evolving and the domain size remained polydisperse. Thus, the question of the stability of finite-sized domains at the air–water interface remains unresolved. Experiments

designed at probing the path to true equilibrium structures are currently under way.

Immediately following the compression/expansion cycle, as the monolayer surface pressure drops to below the phase transition pressure, the monolayer begins to separate into two fluid phases. The dark phase is rich in DChol as the fluorescent dye used is preferentially partitioned into the lipid-rich phase. The initiation of the phase separation into separate phases is characterized by the simultaneous appearance of microscopic dark domains across the field of view of the microscope (Figure 6). These small domains undergo rapid Brownian motion while their sizes increase rapidly over time. In experiments carried out over many hours, the domains could be seen to grow in size over time (at constant surface pressure) while the number density of the domains decreased (Figure 6). This is in qualitative agreement with theory based on an Ostwald ripening mechanism<sup>11–13</sup> where the dominant mechanism of domain growth is not through coalescence but through the diffusive exchange of individual molecules between domains as they diffuse through the fluidlike matrix. In this process, larger domains grow at the expense of smaller domains until the equilibrium domain size is reached or until phase separation is complete. At the end of the 13 h observation period, the domains were still ripening at a very slow rate. The surface was clean and free of contaminants as indicated by the round shape of the domains and the separation between them. The presence of trace contaminants is likely to cause domains to aggregate or to cause their shape to be irregular. During the entire observation period, the trough was checked for leakage periodically. No significant fluorescence was found on the other side of the barrier, indicating that the trough was tightly sealed.

### Summary and Conclusions

We described the design and calibration of a miniature Langmuir trough and a wire loop tensiometer for surface pressure measurements. When used together, they permit prolonged experiments on the microscopic properties of monolayers. The small volume and portability of the trough make it a useful tool for studying the interactions of biological molecules under well-controlled solution and environmental conditions. Improvements in the fabrication of the wire loop tensiometer should allow for surface pressures to be measured with an accuracy of 0.22 mN/m. We find that monolayer domains are probably not equilibrium structures and that they slowly grow via an Ostwald ripening mechanism over periods of many hours. Attempts are now under way to probe the true equilibrium domain morphology.

**Acknowledgment.** The authors thank Ci Lu, Bob Hill, and Greg Carver for assistance in machining the trough components. We also thank Timothy Radsick for helpful discussions on solid mechanics calculations. This work was supported by National Institutes of Health Grant No. 8 R01 EB 00380-09.

LA026372Y